CrossMark

ORIGINAL ARTICLE

Reproducibility and clinical potential of myocardial mass at risk calculated by a novel software utilizing cardiac computed tomography information

Satoru Sumitsuji[1] · Seiko Ide[1] · Patrick T. Siegrist[1] · Youssef Salah[1] ·
Kensuke Yokoi[1] · Masatoki Yoshida[2] · Masaki Awata[1] · Keita Yamasaki[1] ·
Kouichi Tachibana[1] · Hideaki Kaneda[1,3] · Shinsuke Nanto[4] · Yasushi Sakata[5]

Abstract To select the best revascularization strategy a correct understanding of the ischemic territory and the coronary anatomy is crucial. Stress myocardial perfusion single photon emission computed tomography (SPECT) is the gold standard to assess ischemia, however, SPECT has important limitations such as lack of coronary anatomical information or false negative results due to balanced ischemia in multi-vessel disease. Angiographic scores are based on anatomical characteristics of coronary arteries but they lack information on the extent of jeopardized myocardium. Cardiac computed tomography (CCT) has the ability to evaluate the coronary anatomy and myocardium in one sequence, which is theoretically the ideal method to assess the myocardial mass at risk (MMAR) for any target lesion located at any point in the coronary tree. In this study we analyzed MMAR of the three main coronary arteries and three major side branches; diagonal (Dx), obtuse marginal (OM), and posterior descending artery (PDA) in 42 patients with normal coronary arteries using an algorithm based on the Voronoi method. The distribution of MMAR among the three main coronary arteries was 44.3 ± 5.6 % for the left anterior descending artery, 28.2 ± 7.3 % for the left circumflex artery, and 26.8 ± 8.6 % for the right coronary artery. MMAR of the three major side branches was 11.3 ± 3.9 % for the Dx, 12.6 ± 5.2 % for the OM and 10.2 ± 3.4 % for the PDA. Intra- and inter-observer analysis showed excellent correlation ($r = 0.97$; $p < 0.0001$ and $r = 0.95$; $p < 0.0001$, respectively). In conclusion, CCT-based MMAR assessment is reliable and may offer important information for selection of the optimal revascularization procedure.

Keywords Myocardial mass at risk · Cardiac computed tomography · Voronoi method

Introduction

The extent and severity of inducible ischemia, as measured by stress myocardial perfusion single photon emission computed tomography (SPECT), provides independent prognostic information in patients with ischemic heart disease [1–3]. Therefore, SPECT is commonly used for risk stratification and therapeutic decision making in patients with known or suspected coronary artery disease [2].

However, SPECT has limitations such as low spatial resolution, need for radioactive tracer injection, artifacts, and underestimation of ischemia in patients with multi-vessel disease due to the phenomenon of balanced ischemia. More importantly, SPECT does not provide anatomical information on the coronary arteries. Thus, it is difficult to accurately define a specific myocardial territory according to its supplying coronary artery. Although SPECT as well as T2-

S. Sumitsuji and S. Ide contributed equally to this work.

✉ Satoru Sumitsuji
satoru@sumi2g.sakura.ne.jp

1 Department of Advanced Cardiovascular Therapeutics, Osaka University Graduate School of Medicine, 2-2 Yamada Oka, Suita, Osaka 565-0871, Japan

2 Department of Cardiovascular Medicine, Okayama University Graduate School of Medicine, Dentistry and Pharmaceutical Sciences, Okayama, Japan

3 Translational Research Informatics Center, Foundation for Biomedical Research and Innovation, Kobe, Japan

4 Nishinomiya Municipal Central Hospital, Nishinomiya, Japan

5 Department of Cardiology, Osaka University Graduate School of Medicine, Suita, Japan

weighted cardiovascular magnetic resonance and contrast ultrasound cardiography have been shown to correctly estimate the myocardial mass at risk (MMAR) in the setting of an acute coronary occlusion (in an acute coronary syndrome or by balloon inflation) [4–6], the same method cannot be applied for a regular stenosis.

Angiographic scores have been developed to provide prognostic information based on anatomical findings [7, 8]. However, such scoring systems vary in complexity and are not applicable to all patient subsets. Particularly in patients with aberrant vessel anatomy, total occlusions or damaged and thin myocardium such as in an old myocardial infarction, the estimation of perfusion territories would be inaccurate [9].

Hence, the combined angiographic and myocardial information is needed to accurately estimate MMAR. Cardiac computed tomography (CCT), which has emerged as a noninvasive method for direct visualization of coronary artery disease, allows assessment of myocardial mass and coronary lesions in one sequence from which MMAR can be determined.

The concept of using CT data for assessment of tissue volumes perfused by a particular vessel has recently been applied in patients with hepatic disease to determine an accurate liver resection volume. Based on Voronoi's algorithm, a novel simulation software for CT analysis reliably defined vascular perfusion volumes according to the 3D course and diameter of portal veins [10]. A similar segmentation method, which defines perfusion territories according to direction and diameter of supplying vessels may be applicable to coronary arteries and myocardium; i.e., for the assessment of MMAR.

The purpose of the present study was to validate a novel software for CCT-based MMAR measurement against previously published cadaver heart data [11]. In addition we sought to evaluate the reproducibility of the software by means of intra-observer and inter-observer variability.

Method

Patients

MMAR of the major coronary arteries and main side branches as well as the reproducibility of MMAR measurements were assessed in 42 patients who underwent CCT for evaluation of ischemic heart disease between November 2012 and January 2013. All patients had normal coronary arteries and no history of previous myocardial infarction. Patients with hypoplastic right coronary artery (RCA) without posterior descending artery (PDA) were excluded. All CCT examinations had good image quality.

CCT image acquisition

All CCT images were obtained using an Aquilion ONE computed tomography scanner (Toshiba Medical systems, Otawara, Japan) with 0.5-mm detector elements, 350 ms of gantry rotation time, and up to 16 cm of coverage in the Z direction. Tube voltage and current were adapted to body weight (BW) and thoracic anatomy. A nonionic contrast medium (Iomeron 350; Eisai, Tokyo, Japan) was injected at 4–5 ml/s to a total of $0.75 \times$ BW. According to the bolus tracking technique, a threshold was set at 200 HU in the ascending aorta. Automatic reconstruction was performed using the vendor-specific software (Phase NAVI) [12] to determine the optimal phase of images (retrospective ECG-triggering). All datasets were reconstructed with a slice thickness of 0.5 mm and a reconstruction increment of 0.25 mm.

Image processing and calculation of MMAR

Standard DICOM data were transferred to a Ziostation 2 (Zio soft Inc., Tokyo, Japan) incorporating the novel software to calculate MMAR. The algorithm used in this software is based on the Voronoi method [13] upon which the left ventricular myocardium is partitioned into perfusion volumes according to their distance to the closest supplying coronary artery. A 3D reconstruction of the coronary arteries and left ventricular (LV) myocardium was computed after automatic and additional manual tracing of all visible coronary branches.

After setting a specific point in the coronary artery tree (representing a potential lesion), the corresponding myocardial volume was calculated by including all voxels distal to the point and closer to that compromised coronary artery than any other (Fig. 1). MMAR was then calculated automatically as the percentage of the corresponding myocardium in relation to the total LV myocardial mass.

In this study the specific points were set at the ostium of each of the three main coronary arteries: RCA, left anterior descending artery (LAD), left circumflex artery (LCX) and their major side branches: main diagonal branch (Dx), main obtuse marginal branch (OM), and PDA.

Major side branches were defined according to the American Heart Association guidelines [14]: Dx being the branch originating from the proximal LAD covering the anterior wall; OM being the branch of the proximal LCX running along the anterolateral wall; and PDA being the branch of the distal RCA running in the posterior interventricular groove providing septal branches.
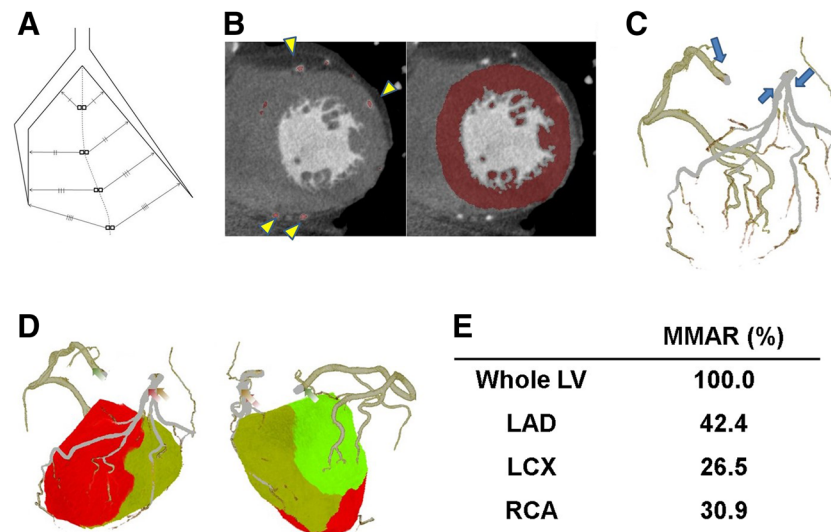
Fig. 1 Segmentation algorithm and how to use the software. **a** The software recognizes the left ventricular myocardium as well as the coronary arteries and their branches by automatic and additional manual tracing. Each voxel of the left ventricular myocardium is allocated to the nearest main coronary artery according to its distance from the coronary artery branches. **b** For calculation of the 3D layout of the coronary arteries (*arrow heads*) and the *left* ventricle, the software uses digital imaging and communication in medicine (DICOM) data of cardiac CT. **c** In the 3D layout of the coronary arteries target points (*arrows*), resembling possible coronary stenoses, can be set manually. In the present case, the target points were set on the origin of the main coronary arteries. **d** Color map of MMAR as calculated by the 3D layout of the coronary arteries and their corresponding myocardium; LAD in *red*, LCX in *yellow* and RCA in *green*. **e** MMAR percentage of the main coronary arteries relative to the whole LV mass

Intra- and inter-observer analysis

MMAR measurements of the first 14 patients were performed independently by two cardiologists experienced in CCT analysis. Inter-observer analysis was performed for MMAR measurements of all three main coronary arteries and the three major branches. One of the observers repeated the analysis more than one month later to assess the intra-observer variability.

Statistical analysis

Statistical analysis was performed using the JMP software (v.11 for Windows; SAS Institute Inc., NC, USA). Quantitative variables were expressed as mean ± standard deviation. The inter-observer and intra-observer agreement for the MMAR measurements were examined using Pearson's correlation coefficient (r) and Bland–Altman analysis with limits of agreement. A p value of <0.05 indicated a statistically significant difference.

Results

Patient characteristics are presented in Table 1.

24 out of 42 patients were male. The mean age was 67.5 years. All CT images were acquired in diastolic phase.

Table 1 Patient characteristics

	Total	Intra- inter-observer
N	42	14
Male/female	24/18	8/6
Age (years)	67.5 ± 13.9	70.4 ± 19.6
Hypertension	26 (61.9%)	9 (64.3%)
Dyslipidemia	18 (42.9%)	5 (35.7%)
Diabetes mellitus	7 (16.7%)	2 (14.3%)
Smoking	13 (31.0%)	2 (14.3%)
Family history of CAD	2 (4.8%)	0
Suspicion of ACS	3 (7.1%)	2 (14.3%)
Suspicion of effort angina	15 (35.7%)	6 (42.9%)
Suspicion of SMI	23 (54.8%)	6 (42.9%)
Heart rate (bpm)	58.9 ± 12.1	61.9 ± 7.7

Presented as N (%), mean ± SD

CAD Coronary artery disease, *ACS* acute coronary syndrome, *SMI* silent myocardial ischemia

The result of the automatic and additional manual tracking of the coronary arteries, the LV myocardium tracing as well as the color map of the MMAR analysis are displayed in Fig. 1.

MMAR measurements are shown in Table 2. The mean percentage of MMAR was 72.5 ± 8.5 % for the entire left coronary artery (95 % CI 69.8–75.1 %), 44.3 ± 5.6 % for

Table 2 MMAR of the main coronary arteries and major side branches

Target	Average ± SD (%)	95% CI (%)
LCA	72.5 ± 8.5	69.8–75.1
LAD	44.3 ± 5.6	42.6–46.1
LCX	28.2 ± 7.3	25.9–30.4
RCA	26.8 ± 8.6	24.2–29.5
Dx	11.3 + 3.9	10.1–12.5
OM	12.6 + 5.2	11.0–14.2
PDA	10.2 + 3.4	9.2–11.3

the LAD (95 % CI 42.6–46.1 %), 28.2 ± 7.3 % for the LCX (95 % CI 25.9–30.4 %), and 26.8 ± 8.6 % for the RCA (95 % CI 24.2–29.5 %).

Among the major side branches, the Dx accounted for 11.3 ± 3.9 % (95 % CI 10.1–12.5 %), the OM for 12.6 ± 5.2 % (95 % CI 11.0–14.2 %) and the PDA for 10.2 ± 3.4 % (95 % CI 9.2–11.3 %) of the total LV myocardium.

Reproducibility of MMAR measurement

Intra-observer and inter-observer variability were excellent ($r = 0.97$; $p < 0.0001$ and $r = 0.95$; $p < 0.0001$, respectively). The MMAR measurement demonstrated small differences in intra-observer and inter-observer comparisons (−0.02 and −0.23 %, respectively) with narrow limits of agreement, as visualized by the Bland–Altman plots in Fig. 2.

Discussion

Comparison to cadaver heart data

Early studies have documented a direct relation between coronary artery lumen size and LV wall mass or volume of perfused myocardium [15, 16]. A more detailed study in canine hearts found a direct relation between the myocardial volume distal to any point in a coronary artery and the summed length of all arterial branches distal to that point in the coronary tree [9]. In a postmortem study of human hearts, Kalbfleisch et al. assessed the relative amount of myocardium perfused by the three main coronary arteries using radiographies of transverse serial cross-sections of the ventricular myocardium with enhanced coronary arteries for planimetrical measurements [11]. In 129 cases with normal coronary artery type, an average of 62.7 % of the total (i.e., right- and left ventricular) myocardium was supplied by the LCA (41.7 % LAD and 21.0 % LCX). The remaining 37.3 % was supplied by the RCA.

In the present study, the percentage of supplied myocardium relates to the left ventricular mass only. Based on previously published data, where the RV mass accounts for 22.5 % of the total myocardial mass [17] and the RCA supplies 16.4 % of total myocardial mass in left coronary artery dominant type heart [11], and with an assumption of remaining right ventricular (6.1 % of total myocardial mass) is supplied by LAD, our data can be calculated for the total myocardial mass of which the LCA then supplies 62.6 % (40.8 % LAD and 21.8 % LCX) and the RCA for 36.9 %. This is in excellent accordance with the previously reported postmortem data [11].

Validity of this new software

In the present study, we used a novel software to measure MMAR using CCT information of the coronary arteries and the underlying volume of myocardium. The segmentation algorithm, a modification of the Voronoi method, has already been successfully applied for hepatectomy simulation [10]. We sought to apply the same concept to assess the myocardial territory of a corresponding coronary artery. Although the current version of this software needs manual correction for coronary artery and myocardium detection, the inter- and intra-observer data showed good correlation for MMAR measurements of the main vessels and their major branches.

Clinical relevance

Evaluation of MMAR offers three main advantages with clinical relevance.

First, MMAR assessment could be used as an additional factor to influence treatment strategy. While ischemic size as detected by SPECT remains the most important factor for decision making in most patients, MMAR assessment might provide useful additional information in cases of balanced ischemia, inconclusive or unavailable SPECT examination. Furthermore, MMAR assessment provides an objective measurement of the size of the myocardial territory affected by a potential target lesion. In most cases the attending physician's estimation of the extent of compromised myocardium affects the treatment strategy but the reliability of such an estimation remains questionable as it is not based on an objective measurement. MMAR, as assessed by our new software, provides accurate and reproducible values. As exemplified in a case with a large occluded Dx (Fig. 3), the MMAR of the branch is 20.7 %, which almost equals the perfusion territory of the LAD (22.6 %). With this additional information, revascularization of the Dx appears more important compared to an average-sized Dx. MMAR measurements in general have the potential of providing more objective information for
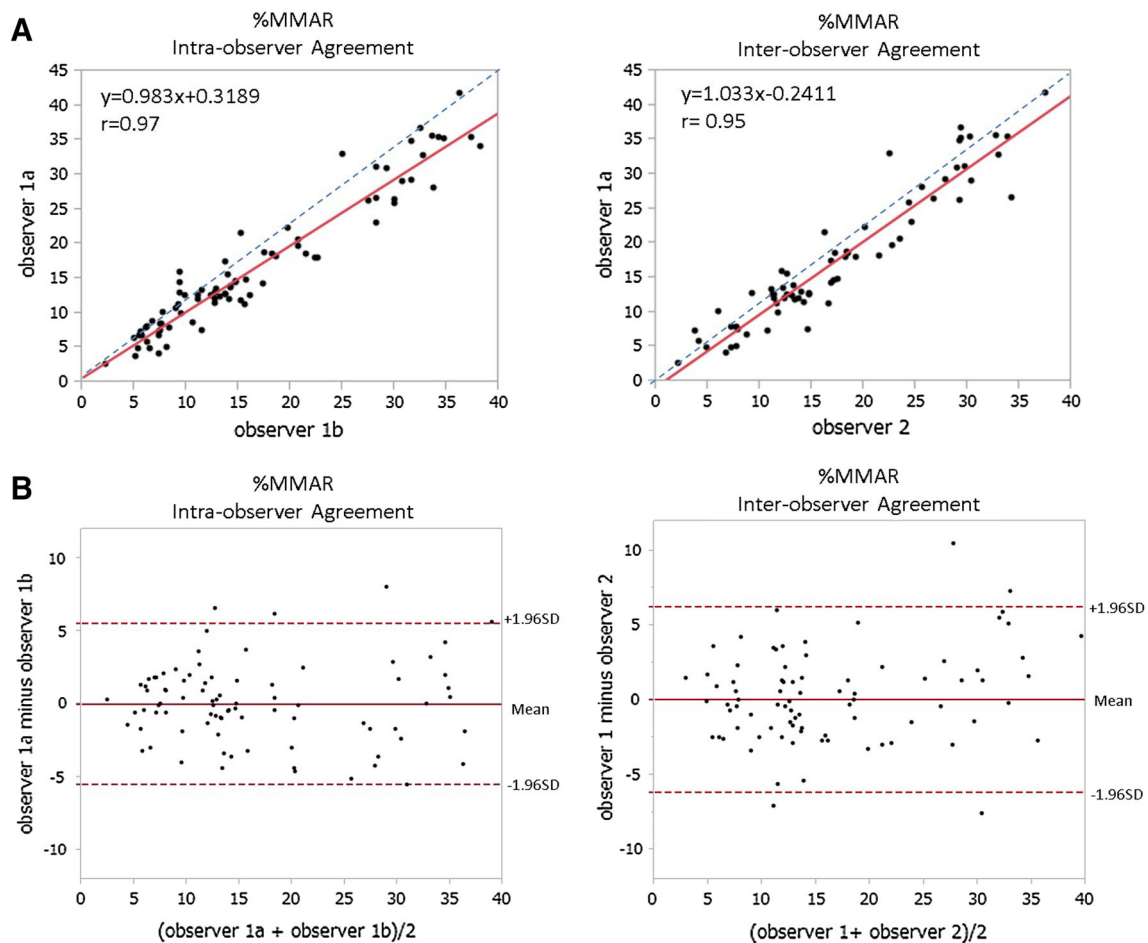
Fig. 2 Validation of MMAR with intra-observer and inter-observer analysis. **a** Intra-observer (*left*) and inter-observer (*right*) correlations of all MMAR measurements (three main arteries, three major branches, $n = 84$). *Trend line* (continuous) and *line* of identity is given in both graphs. **b** Bland–Altman plot illustrating mean intra-observer and mean inter-observer difference for MMAR measurements (*continuous line*). 1.96 SD (*dotted lines*) denotes repeatability coefficient

decision making in cases with complex or aberrant coronary anatomy.

Second, MMAR provides information on the myocardial mass potentially affected by ischemia. As it is already well-known, ischemia is not only determined by stenosis severity but also by the amount of myocardial mass distal to the culprit lesion [18]. The angiography depicted in Fig. 4 shows an intermediate stenosis in the proximal LAD. While the significance of the stenosis was unclear by angiography alone, ischemia was revealed by additional FFR measurement, which surprisingly showed a value of 0.74. Considering the extensive MMAR of 56.8 %, which is considerably larger than that of an average LAD (41.6 % in cadaver heart, 44.3 % in the present study), the functional significance of the angiographically intermediate lesion could have been suspected by CCT.

Third, MMAR has the potential to evaluate myocardium salvage therapy in acute myocardial infarction. Lee et al. reported an excellent correlation between the vascular bed at risk as determined from X-rays of the ventricles after

postmortem injection with barium sulfate and histological infarct size [19]. Moreover they presented that transmural wave front progression of myocardial cell death found in canine hearts could also occur in evolving human infarction. In the third exemplary case presented in Fig. 5, an old myocardial infarction of an OM branch showed excellent agreement between the related wall-thinning area and the software-derived MMAR (colored in red).

Limitations

First, this software applied a segmentation algorithm based on the Voronoi method. Although this segmentation concept has already been successfully applied for hepatectomy procedures, some concerns about adopting this method for the segmentation of myocardium remain. Nevertheless, myocardial perfusion volumes of the supplying coronary arteries assessed in our study had a very similar distribution compared to previously published studies using cadaver

Reproducibility and clinical potential of myocardial mass at risk calculated by a novel...

223

Fig. 3 A case with an occluded large diagonal branch. **a** Coronary angiogram in LAO cranial projection. A large diagonal branch is totally occluded from the ostium (*arrow head*). **b** Coronary angiogram of the right coronary artery shows retrograde perfusion of the occluded diagonal branch via collaterals. **c** Color map of MMAR assessment. The territory of the LAD is shown in *red* and the territory of the occluded diagonal branch in *yellow*. **d** Expressed as percentage of the total LV mass, MMAR of the diagonal branch (20.7 %) almost equaled the perfusion territory of the remaining LAD (22.6 %)
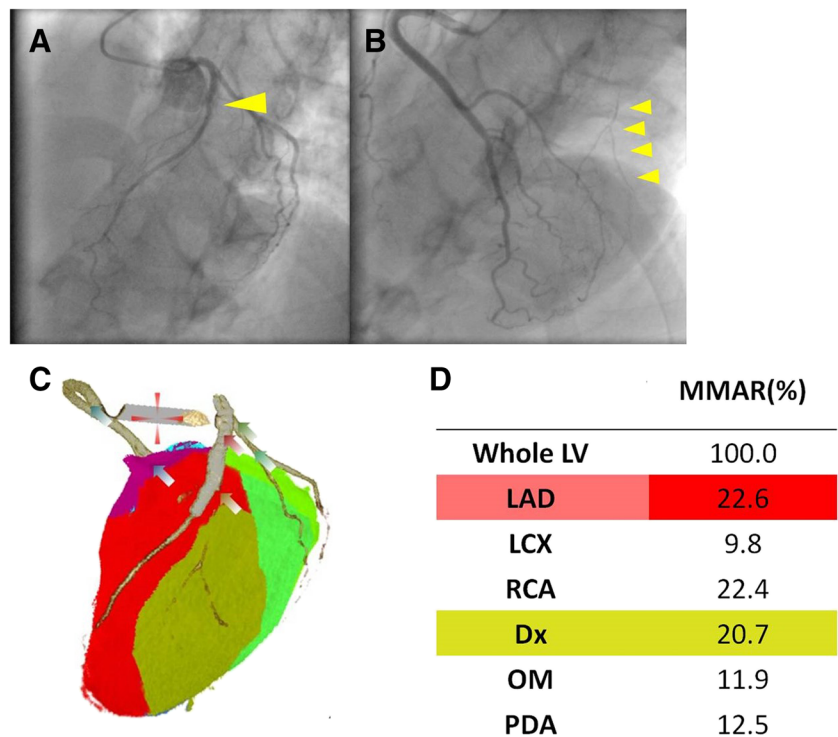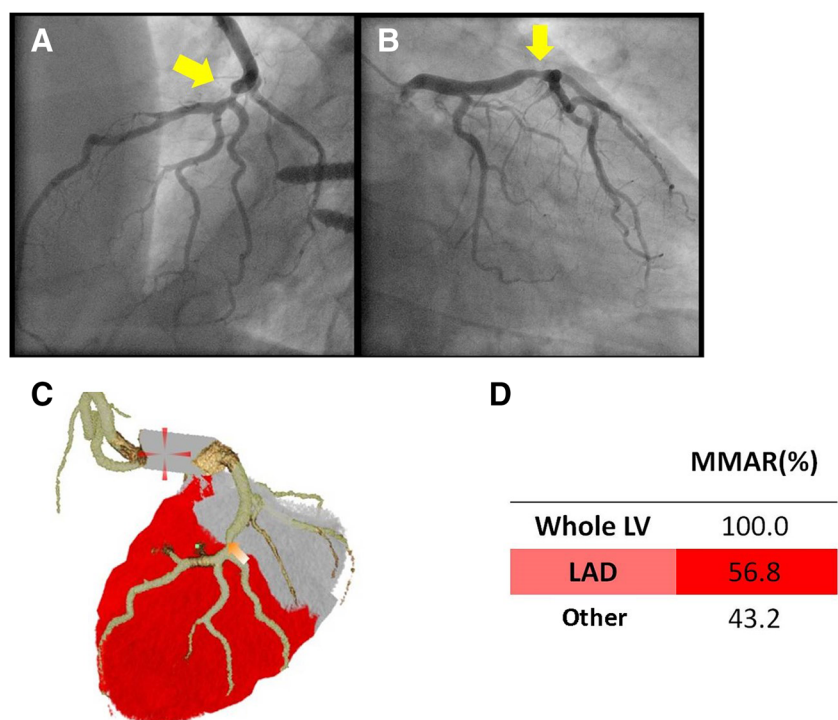
	MMAR(%)
Whole LV	100.0
LAD	22.6
LCX	9.8
RCA	22.4
Dx	20.7
OM	11.9
PDA	12.5

Fig. 4 A case with an intermediate stenosis in the proximal *left* anterior descending artery. **a** Coronary angiogram of the *left* coronary artery in the left anterior oblique (LAO) cranial projection depicts an intermediate stenosis in the proximal LAD. **b** Coronary angiogram in the *right* anterior oblique (RAO) caudal projection confirmed the intermediate stenosis in the proximal LAD. **c** Color map of MMAR assessment. The large territory affected by the proximal LAD lesion is shown in *red*. **d** In the present case the MMAR of the proximal LAD lesion (56.8 %) was larger than the average MMAR of a full LAD (42.6 ± 6.3 % in our study)

	MMAR(%)
Whole LV	100.0
LAD	56.8
Other	43.2

hearts. For further clarification we are currently conducting a validation study in swine hearts.

A second important concern is the consistency of MMAR measurements by this new method. In the present study coronary arteries were traced as far as possible by using the diastolic phase. Insufficient tracing of coronary arteries or applying other cardiac cycles might influence MMAR values. Further studies should be conducted to elucidate this concern.

Third, in cases with well-developed collateral channels, accurate determination of MMAR would be difficult. In fact, when CT detects connection between coronary
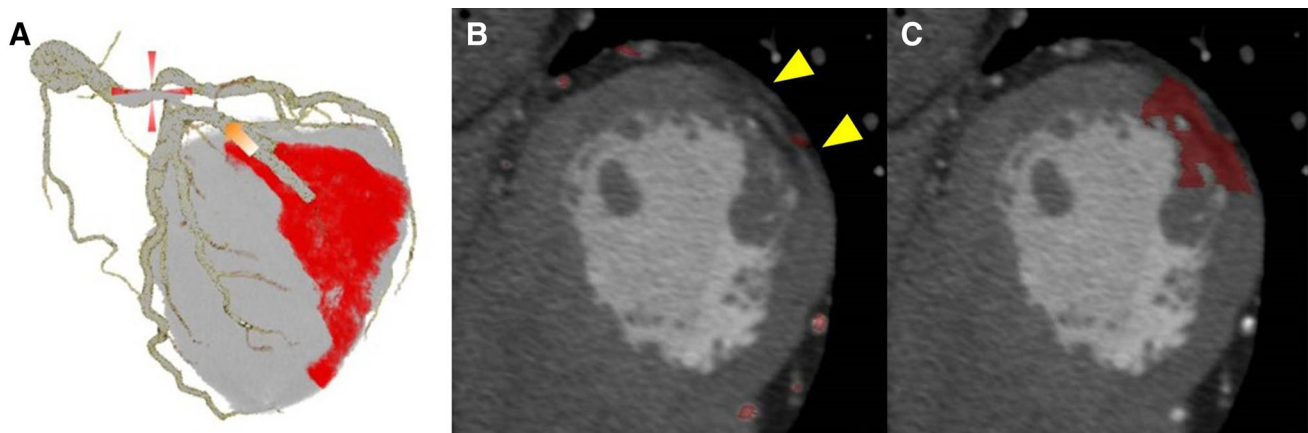
Fig. 5 A case of an old myocardial infarction due to occlusion of the obtuse marginal branch. **a** *Color map* of MMAR assessment. The territory of the obtuse marginal branch is shown in *red*. **b** The infarcted area presented with typical myocardial thinning and low CT attenuation. **c** The *red colored* MMAR correlated well with the corresponding infarcted area

arteries, this software cannot calculate exact territory mass due to incomplete or failure of segmentation. Such cases should not be target of this assessment.

Lastly, the relationship between MMAR and ischemic size as detected by SPECT is still not well evaluated. Kurata et al. [20] showed good correlation between MMAR and comprehensive summed stress score/summed difference score, especially in severe single vessel disease, but the number of patients was limited. Therefore, when using MMAR values to decide treatment strategy, an additional proof of ischemia should still be considered.

Conclusion

Assessment of MMAR using CCT data and a novel software with a dedicated segmentation algorithm provided reproducible values which were well comparable to previously reported data of cadaver hearts. MMAR measurement has a potential to improve treatment decision, predict ischemia, and evaluate the efficacy of myocardium salvage treatment.

Compliance with ethical standards

References

1. Hachamovitch R, Berman DS, Shaw LJ, Kiat H, Cohen I, Cabico JA, et al. Incremental prognostic value of myocardial perfusion single photon emission computed tomography for the prediction of cardiac death: differential stratification for risk of cardiac death and myocardial infarction. Circulation. 1998;97(6):535–43.

2. Shaw LJ, Berman DS, Maron DJ, Mancini GB, Hayes SW, Hartigan PM, et al. Optimal medical therapy with or without percutaneous coronary intervention to reduce ischemic burden: results from the clinical outcomes utilizing revascularization and aggressive drug evaluation (COURAGE) trial nuclear substudy. Circulation. 2008;117(10):1283–91.

3. Zellweger MJ, Hachamovitch R, Kang X, Hayes SW, Friedman JD, Germano G, et al. Threshold, incidence, and predictors of prognostically high-risk silent ischemia in asymptomatic patients without prior diagnosis of coronary artery disease. J Nucl Cardiol. 2009;16(2):193–200.

4. Pereztol-Valdes O, Candell-Riera J, Oller-Martinez G, Aguade-Bruix S, Dastell-Conesa J, Angel J, et al. Localization and quantification of myocardium at risk by myocardial perfusion SPECT during coronary artery occlusion. Rev Esp Cardiol. 2004;57:635–43.

5. Wincw WB, Kim RJ. Molecular imaging: T2-weighted CMR of the area at risk-a risky business? Nat Rev Cardiol. 2010;7:547–9.

6. Lafitte S, Higashiyama A, Masugata H, Peters B, Strachan M, Kwan OL, et al. Contrast echocardiography can assess risk area and infarct size during coronary occlusion and reperfusion: experimental validation. J Am Coll Cardiol. 2002;39(9):1546–54.

7. Alderman EL, Stadius M. The angiographic definitions of the bypass angioplasty revascularization investigation. Coron Artery Dis. 1992;3:1189–207.

8. Graham MM, Faris PD, Ghali WZ, Galbraith PD, Norris CM, Badry JT, et al. Validation of three myocardial jeopardy scores in a population-based cardiac catheterization cohort a population-based cardiac catheterization cohort. Am Heart J. 2001;142(2):254–61.

9. Seiler C, Kirkeeide RL, Gould L. Measurement from arteriograms of regional myocardial bed size distal to any point in the coronary vascular tree for assessing anatomic area at risk. J Am Coll Cardiol. 1993;21(3):783–97.

10. Saito S, Yamanaka J, Miura K, Nakao N, Nagao T, Sugimoto T, et al. A novel 3D hepatectomy simulation based on liver circulation: application to liver resection and transplantation. Hepatology. 2005;41(6):1297–304.

11. Kalbfleisch H, Hort W. Quantitative study on the size of coronary artery supplying areas postmortem. Am Heart J. 1977;94(2):183–8.

12. Cho YJ, Choe YH, Lee MS. Comparison of image quality of 64-slice multidetector CT coronary CT angiography using

automated and manual multiphase methods for the determination of optimal phases for image reconstruction in patients with various mean heart rates. Int J Cardiovasc Imaging. 2010;26:41–52.

13. Guibas L, Stolfi J. Primitives for the manipulation of general subdivisions and the computations of Voronoi diagrams. ACM Trans Graph. 1985;4:74–123.

14. Austen WG, Edwards JE, Frye RL, Gensini GG, Gott VL, Griffith LS, et al. A reporting system on patients evaluated for coronary artery disease. Report of the Ad Hoc Committee for Grading of Coronary Artery Disease, Council on Cardiovascular Surgery, American Heart Association. Circulation. 1975;51:5–40.

15. Lewis BS, Gotsman MS. Relation between coronary artery size and left ventricular wall mass. Br Heart J. 1973;35(11):1150–3.

16. Koiwa Y, Bahn RC, Ritman EL. Regional myocardial volume perfused by the coronary artery branch: estimation in vivo. Circulation. 1986;74(1):157–63.

17. Lorenz CH, Walker ES, Morgan VL, Klein SS, Graham TP. Normal human right and left ventricular mass, systolic function, and gender difference by cine magnetic resonance imaging. J Cardiovasc Magn Reson. 1999;1:7–21.

18. Leone AM, De Caterina AR, Basile E, Gardi A, Laezza D, Mazzari MA, et al. Influence of the amount of myocardium subtended by a stenosis on fractional flow reserve. Circ Cardiovasc Interv. 2013;6(1):29–36.

19. Lee JT, Ideker RE, Reimer KA. Myocardial infarct size and location in relation to the coronary vascular bed at risk in man. Circulation. 1981;64(3):526–34.

20. Kurata A, Kono A, Sakamoto T, Kido T, Mochizuki T, Higashino H, et al. Quantification of the myocardial area at risk using coronary CT angiography and Voronoi algorithm-based myocardial segmentation. Eur Radiol. 2015;25(1):49–57.